# Simulation of Respiration-Induced $B_0$ Shifts in the Heart

Anjali Datta[1], Reeve Ingle[1], Bob Hu[1,2], and Dwight Nishimura[1]
[1]*Electrical Engineering, Stanford University, Stanford, California, United States,* [2]*Cardiology, Palo Alto Medical Foundation, Palo Alto, California, United States*

**Introduction:** Respiration-induced $B_0$ variations are of interest because they may lead to off-resonance artifacts in free-breathing acquisitions and may contribute to variable image quality across patients. Studies have shown that changes in the air volume in the lungs and the movement of the chest and diaphragm during respiration induce susceptibility-dependent fluctuations that contribute significant noise in brain fMRI.[1,2] In addition, respiration-induced resonance offsets are the primary source of artifacts in breast MR spectroscopy due to the closeness to the lungs.[3] Despite the proximity of the heart to the lungs, the effects on cardiac imaging have not, to our knowledge, been previously examined due to the predominance of breath-hold scans. Using a computational phantom to generate susceptibility models, we simulate the main field map over the heart in several respiratory frames and in different anatomies to determine if $B_0$ variations across the breathing cycle and between individuals may be significant.

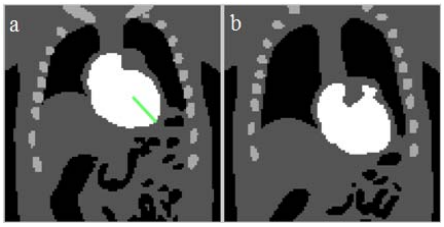


**Figure 1.** Coronal slices (cropped) of the model with air (black), soft tissue (dark gray), bone (light gray), and the heart (white). **(a)** Plane at end expiration with LV long axis (at 52°) shown in green. **(b)** Same plane at end inspiration.

**Methods:** The XCAT1 4D computational phantom developed by Segars, et al.[4] was used to generate voxel susceptibility models of the head, arms, and torso with 3.75 mm isotropic spatial resolution. The following susceptibility assumptions were made based on Koch, et al.[5]: lungs and other air cavities, $\chi = 0.3\text{x}10^{-6}$; bones, $\chi = -11.4\text{x}10^{-6}$; all other tissues, $\chi = -9.2\ \text{x}10^{-6}$. Models were created with left ventricular (LV) long-axis orientations of 52° and 35° in the coronal plane at end expiration to correspond to average values reported by Foster, et al.[6] in healthy volunteers and chronic heart failure patients, respectively. The extent of translation of the heart simulated during respiration corresponded to the mean values found by Shechter, et al.[7]: S/I, -4.9 cm; A/P, 1.2 mm; L/R, 0.4 mm. The mean values for the rotation of the heart between end expiration and end inspiration (cranio-dorsal: 1.6°, caudo-dextral: 1.4°, posterior-dextral: 0.8°)[7] were incorporated into the phantom's movement. Over the respiratory cycle of 5 s (2 s inspiration and 3 s expiration), the change in motion parameters was defined by

$$\Delta\, a(t) = \begin{cases} a_{max}[1-\cos(\pi t/2)], 0 \le t < 2 \\ a_{max}[1-\cos(\pi(5-t)/3)], 2 \le t < 5 \end{cases}$$

Ten respiratory frames were analyzed (0.5 s temporal resolution). A Fourier-transform-based solution for the dipole approximation of $B_{in}$, which is the perturbation of the main field induced by an arbitrary susceptibility distribution (within the small susceptibility limits of materials in humans),[5,8,9] was used to efficiently compute the field map corresponding to each respiratory position of the voxel models. The linear least-squares fit for $B_{in}$ values over the heart in the end expiration frame was subtracted from all ten frames to mimic linear gradient shimming. The shimmed $B_{in}$ maps were then translated and rotated so that the change in the induced field with respiration, $\Delta B_{in}$, could be calculated in the reference field of the heart. The optimal first-order-compensated field map at end inspiration was additionally computed to compare field homogeneity after shimming at end expiration and end inspiration.

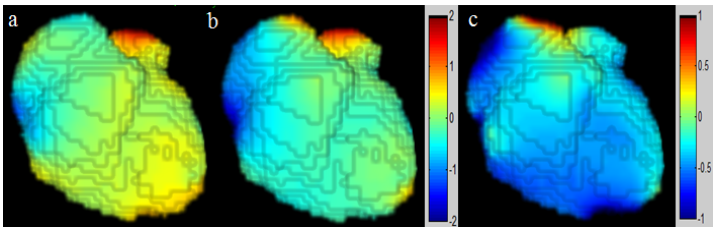


**Figure 2.** Surface plots of the $B_0$ field (in ppm) over the heart at 52° LV orientation. **(a)** $B_{in}$ at end expiration. **(b)** $B_{in}$ at end inspiration. **(c)** $\Delta B_{in}$ (inspiration–expiration).

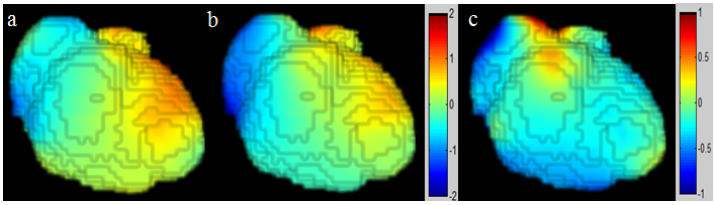


**Figure 3.** Surface plots of the $B_0$ field (in ppm) over the heart at 35° LV orientation. **(a)** $B_{in}$ at end expiration. **(b)** $B_{in}$ at end inspiration. **(c)** $\Delta B_{in}$ (inspiration–expiration).

**Results:** The field maps at end expiration and end inspiration (with LV long-axis orientation of 52°) shown in Figure 2(a-b) have standard deviations of 0.405 and 0.509 ppm (25.9 and 32.5 Hz at 1.5 T), respectively. This is after first-order shimming based on end expiration. When shimmed at end inspiration, $B_{in}$ at this respiratory position has a standard deviation of 0.501 ppm (32.0 Hz at 1.5 T). The difference map in Figure 2(c) shows an overall decrease in the field strength during inspiration, although the magnitude of the change is spatially variant. $\Delta B_{in}$ has a mean of -0.487±0.227 ppm (-31.1±14.5 Hz at 1.5 T). Figure 3 shows the shimmed $B_{in}$ at end expiration, inspiration, and $\Delta B_{in}$ between the two for LV orientation of 35°. The standard deviations of the induced field perturbations are similar to those at 52° (0.412 ppm at end expiration and 0.513 ppm at end inspiration), but the spatial distributions are different and the respiration-induced field shift is smaller, with mean -0.334±0.209 ppm (-21.3±13.3 Hz at 1.5 T).

**Discussion and Conclusion:** The better homogeneity (lower standard deviation) of the shimmed end-expiration field compared to the shimmed end-inspiration field may be justification for acquiring breath-hold scans at end expiration, as is typically done. This work suggests that respiration induces spatially-variant $B_0$ shifts in the heart and that the magnitude and distribution of $\Delta B_{in}$ depend on the LV axis orientation. Future work includes in-vivo field mapping studies to verify the simulation results. If the results are confirmed, they suggest that more sophisticated off-resonance correction techniques may need to be performed for free-breathing cardiac imaging, especially for non-Cartesian acquisitions. This could include using field maps at several respiratory positions for respiration-dependent off-resonance correction. In conclusion, we have simulated the $B_0$ shifts over the respiratory cycle caused by lung volume changes and chest movement in a 4D computational phantom.

**References:** [1] Van de Moortele PF, et al. Magn Reson Med. 2002; 47:888–895. [2] Raj D, et al. Phys Med Biol. 2000; 45(12):3809–3820. [3] Bolan PJ, et al. Magn Reson Med. 2004; 52:1239–1245. [4] Segars WP, et al. Med Phys. 2010; 37:4902–15. [5] Koch KM, et al. Phys Med Biol. 2006; 51:6381–6402. [6] Foster JE, et al. Clin Physiol Funct Imaging. 2005 Sep; 25(5):286-92. [7] Shechter G, et al. IEEE Trans Med Imaging. 2004; 3:1046–1056. [8] Salomir R, et al. Concepts Magn Reson. 2003; 19B:26–34. [9] Marques JP, Bowtell R. Concepts Magn Reson. 2005; 25B:65–78.